Available online at www.sciencedirect.com
SCIENCE DIRECT®
International Journal of Heat and Mass Transfer 47 (2004) 4243–4255
International Journal of HEAT and MASS TRANSFER
www.elsevier.com/locate/ijhmt

Verification solution for partial heating of rectangular solids

James V. Beck [a,*], A. Haji-Sheikh [b], Donald E. Amos [c,1], David Yen [d]

[a] Department of Mechanical Engineering, Michigan State University, East Lansing, MI 48824, USA
[b] Department of Mechanical and Aerospace Engineering, The University of Texas at Arlington, 500 West First St, Arlington, TX 76019-0023, USA
[c] Sandia National Laboratories, Albuquerque, NM 87110, USA
[d] Department of Mathematics, Michigan State University, East Lansing, MI 48824, USA

Received 15 March 2004; received in revised form 30 April 2004

Abstract

One method for verification of numerical solutions in heat transfer uses exact solutions for multi-dimensional parallelepipeds. The usual solution of these problems utilizes the method of separation of variables for both the steady and transient parts of the solution; however, this method for the steady-state part often produces solutions that converge slowly at the boundaries of greatest interest. Steady-state solutions having low convergence are illustrated for a rectangle with zero prescribed temperatures except one surface having a step change of temperature. Two forms of the steady-state solution are available and even then difficulties may be encountered. Another method called time-partitioning is used and is shown to have several superior features in the solution of this problem.
© 2004 Elsevier Ltd. All rights reserved.

1. Introduction

Verification of approximate numerical solution methods is an important process in assuring accurate and reliable numerical values for numerous heat transfer problems. Approximate solution methods include finite difference, finite control volume and finite element methods. One method for verification uses manufactured solutions [1]; it is important when solving coupled non-linear partial differential equations, such as in convection problems. A disadvantage is that sources or sinks may be needed in this method. A related method constructs a non-linear solution for a prescribed temperature-dependent variation of thermal properties and accepts arbitrary boundary and/or initial conditions [2]; this verification solution does not require sources to complete the solution.

The verification procedure in this paper provides solutions (accurate to any desired level) for the linear 2D or 3D transient heat conduction equation for simple prescribed boundary and initial conditions and also volumetric energy generation. In the method described here, the problems are prescribed and no arbitrary sources or sinks are needed nor are the boundary conditions arbitrary, as in manufactured solutions. However, the geometries are simple and the problem is linear. These solutions are exact for a large number of prescribed problems in steady and transient heat conduction in plates, rectangles and parallelepipeds.

In obtaining verification solutions, a number of features are desirable. These features are now listed for the cases mentioned above:

1. provide extremely accurate values of the temperature and the heat flux components,
2. give large improvements in accuracy without excessive computational cost or change in procedure,
3. treat the three basic boundary conditions for finite and semi-infinite bodies,
4. use the same basic 1D building blocks for all 1D, 2D and 3D steady and transient cases,

* Corresponding author. Tel.: +1-517-349-6688; fax: +1-517-353-1750.
E-mail address: beck@egr.msu.edu (J.V. Beck).
[1] Retired.

0017-9310/$ - see front matter © 2004 Elsevier Ltd. All rights reserved.
doi:10.1016/j.ijheatmasstransfer.2004.04.021

Nomenclature

A_n	steady-state component given by Eq. (7b)
B	boundary condition modifier in conduction notation, Section 2
B_i	coefficient defined by Eq. (18)
C	accuracy constant for maximum value of exponent, Eq. (8b)
C_k	coefficient defined by Eq. (A.2a)
G_{XIJ}	Green's function for boundary conditions of the Ith and Jth kinds, m^{-1}
L	length of rectangle in x-direction, m
L_1	length of region with $T = T_W$, m
n'	outward pointing normal, m
t	time, s
t_p	partition cotime, s
T	temperature, K
T^L	long cotime temperature component, K
T^S	short cotime temperature component, K
$T^L_{c.t.}$	complementary transient temperature, K
q	heat flux, W/m^2
q^S	short cotime component of heat flux, W/m^2
q^L	long cotime component of heat flux, W/m^2
u	cotime, $t - \tau$, s
w_i	length defined in Eq. (19), m
W	length of rectangle in y-direction, m
x, y	coordinates, m
X, Y	notation for conduction problem description, Section 2

5. treat near corners and partial heating on a surface,
6. treat both very small times (semi-infinite behavior) and large times (steady state),
7. permit extension to other coordinates and
8. allow extension to other related problems such as for solid body flow [3,4].

Two bonus features provided by the time-partitioning method are

1. internal verification of the solution method and
2. internal indication of the accuracy.

In Ref. [5], the time-partitioning solution method contains most if not all of these features. In particular the fifth one of treating near corners and partial heating is not addressed. Also the method given in [5] employs numerical integration on time while this paper provides exact integrations for the problem considered. Objectives of this paper include illustrating the power to treat corners/partial heating and to provide exact integrations. Another objective is to contrast the time-partitioning method with more classical approaches using separation of variables, which may provide oscillatory heat fluxes on the heated surfaces.

The time-partitioning method for multi-dimensional heat conduction problems in Cartesian coordinates is based on the use of tabulated 1D Green's functions for a plate [7]. Three basic boundary conditions are considered: prescribed temperature (Dirichlet), prescribed heat flux (Neumann) and prescribed ambient temperature in a convective condition (Robin). It is convenient to call them boundary conditions of the first, second and third kinds, respectively. In so doing, a convenient numbering system can be devised [7]. With these boundary conditions, nine different combinations can be given for a finite, 1D plate. For a thermally semi-infinite region, it is convenient to introduce the boundary condition of the zeroth kind which is for cases at which no physical boundary exists such as at infinity. (See further explanation in Section 2.) In order to numerically solve the transient conduction problem in an efficient way, the time-partitioning method utilizes two sets of Green's functions for the nine basic cases for a finite, 1D plate. One set comes from the Laplace transform and the other from the method of separation of variables. The former is better used for "short" values of $u \equiv t - \tau$ and the latter is best used for "long" values of u; this variable is called "cotime" herein. ("Short" and "long" are defined below with reference to a certain Fourier number.) In addition to the set of nine finite-body 1D Green's functions, many are available for semi-infinite bodies [7].

Exact solutions of steady-state and transient conduction problems commonly employ the method of separation of variables. Although it is a powerful method, in 2D and 3D problems it may not produce accurate numerical values at non-homogenous surfaces. To circumvent this problem, different forms of the solution are available using variation of parameters, steady-state Green's functions and other methods. However, these may have poor convergence properties at a homogeneous surface. This paper illustrates these weaknesses of the classical method of separation of variables and also presents approaches using time-partitioning that do not have these weaknesses.

Appropriate exact methods can be very effective for obtaining extremely accurate and reliable numerical values for the temperature and the heat flux components. Also, the accuracy can readily be improved with relatively modest increased computation. For example, going from 5 digit accuracy to 10 digits in one case herein requires only twice as much computation while it is extremely difficult to get 5-digit accuracy using the finite element and related methods.

In order to focus attention on the time-partition methods and convergence problems in the separation of variables method for transient heat conduction, a simple steady-state problem of a rectangle with temperature boundary conditions is first discussed. Several methods are given for computing the heat flux at a surface with non-homogenous boundary conditions. In the separation of variables method for transient heat conduction problems, transient and steady-state components are usually present. The steady state is given particular attention herein because it is much more difficult to evaluate at the non-homogeneous boundary condition surfaces than is the transient part. However, the time-partitioning method simultaneously yields the steady-state and transient solutions.

2. Separation of variables steady-state solutions

Consider the following 2D steady-state problem, which is denoted $X11B00\ Y11B0(x5)$. Here, X and Y denote the x- and y-directions, respectively; "11" denotes boundary conditions of the first kind at both $x = 0$ and L; B is a boundary condition modifier such that $X11B00$ denotes zero temperatures at $x = 0$ and L; and $Y11B0(x5)$ denotes a zero temperature at $y = 0$ and a step change in the temperature in the x-direction at the $y = W$ surface. If the problem is transient and the initial temperature is zero, we add $T0$ to the notation. (For more description of the numbering system, see [7].) The problem is depicted in Fig. 1 and a mathematical statement of the problem is

$$\frac{\partial^2 T}{\partial x^2} + \frac{\partial^2 T}{\partial y^2} = 0, \quad 0 < x < L, \ 0 < y < W \tag{1}$$

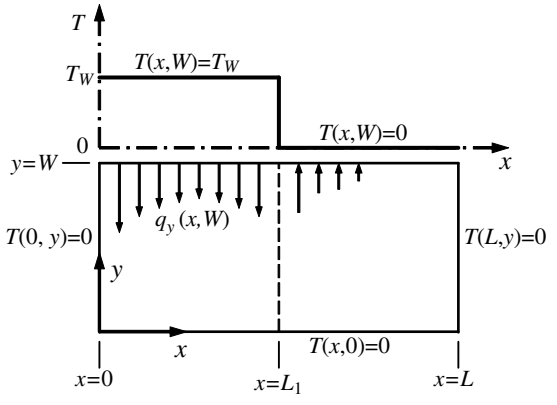

Fig. 1. Steady-state heat conduction problem in a rectangle with zero prescribed temperatures at all surfaces except a temperature of T_W at $y = W$ and $0 < x < L_1$. Problem notation is $X11B00\ Y11B0(x5)$.

$$T(0,y) = T(L,y) = T(x,0) = 0$$
$$T(x,W) = \begin{cases} T_W, & 0 < x < L_1 \\ 0, & L_1 < x < L \end{cases} \tag{2}$$

At $y = W$, the temperature is T_W from $x = 0$ to L_1 and zero from $x = L_1$ to L. Two different solutions can be obtained, one having eigenfunctions in the homogeneous direction (which is x in this problem) and one having eigenfunctions in the y-direction. Ways to derive these two different solutions include separation of variables [7], variation of parameters [8] and Green's functions [9,10].

2.1. Solution using homogeneous-direction (x-direction) eigenfunctions

The classical separation of variables solution is [7]

$$\begin{aligned} \frac{T(x,y)}{T_W} &= \frac{2}{\pi}\sum_{m=1}^{\infty} \sin\left(m\pi\frac{x}{L}\right)\frac{1-\cos(m\pi L_1/L)}{m} \\ &\quad \times \frac{\sinh(m\pi y/L)}{\sinh(m\pi W/L)} \\ &= \frac{2}{\pi}\sum_{m=1}^{\infty} \sin\left(m\pi\frac{x}{L}\right)\frac{1-\cos(m\pi L_1/L)}{m} \\ &\quad \times \frac{e^{-m\pi\frac{W-y}{L}} - e^{-m\pi\frac{W+y}{L}}}{1-e^{-2m\pi\frac{W}{L}}} \end{aligned} \tag{3}$$

which uses the x-direction eigenfunctions. The heat flux components are

$$\begin{aligned} \frac{q_y(x,y)L}{kT_W} &= -2\sum_{m=1}^{\infty} \sin\left(m\pi\frac{x}{L}\right)\frac{\cosh(m\pi y/L)}{\sinh(m\pi W/L)} \\ &\quad \times \left[1-\cos\left(m\pi\frac{L_1}{L}\right)\right] \end{aligned} \tag{4}$$

$$\begin{aligned} \frac{q_x(x,y)L}{kT_W} &= -2\sum_{m=1}^{\infty} \cos\left(m\pi\frac{x}{L}\right)\frac{\sinh(m\pi y/L)}{\sinh(m\pi W/L)} \\ &\quad \times \left[1-\cos\left(m\pi\frac{L_1}{L}\right)\right] \end{aligned} \tag{5}$$

Notice in Eq. (3) for $y = W$ that the ratio of the hyperbolic terms is unity and the denominator contains m to the first power. As a consequence, Eq. (3) converges slowly at $y = W$; although convergence is not a problem because the temperature is known there. The convergence of the heat flux components is much worse; notice that the m in the denominator of Eq. (3) is not present in Eqs. (4) and (5). Both of these heat flux expressions oscillate near $y = W$, the non-homogeneous surface, which is frequently the most important location.

As m becomes large and $y \neq 0$, the $\exp[-m\pi(W-y)/L]$ term decays slower than the other exponential terms in the second form of Eq. (3). This term becomes negligible when the exponent $m\pi(W-y)/L$ is sufficiently large such as $C = 23$, (note that $e^{-23} \approx 1.0E-10$).

Hence the required number of terms for such small errors in the series is

$$m_{\max} = C\frac{L}{\pi(W-y)} = \frac{C}{\pi}\frac{L}{W}\frac{1}{1-y/W}, \quad C \approx 23 \tag{6}$$

which indicates that as y approaches W the number of terms can become extremely large.

We note (for $y \neq W$) that replacing $C = 23$ in Eq. (6) by the smaller value of $C = 23/2 = 11.5$, the error increases to about $1.0\mathrm{E}-5$; hence, increasing C by a factor of two in this case doubles the number of terms but decreases the expected error by a factor of $1.0\mathrm{E}-5$. This contrasts markedly with finite element and other methods for which substantial improvements in accuracy are very costly. On the other hand, finite element methods are clearly more powerful for complex problems.

Fig. 2 shows the dimensionless temperature (given by Eq. (3)) and the dimensionless heat flux (given by Eq. (4)) as functions of the number of terms in the series, M, for $x/L = 0.25$, $y/W = 1$, $L_1/L = 0.5$ and $L/W = 1$. The temperature oscillates about unity with decreasing amplitudes and slowly converges for $M > 40$. For example, for 1000 and 1003 terms in the summation, the computed temperatures are 0.999 and 1.001, respectively. This is not the level of accuracy desired for verification purposes. The heat flux values oscillate between about −0.005 and −6.8, which is unsatisfactory.

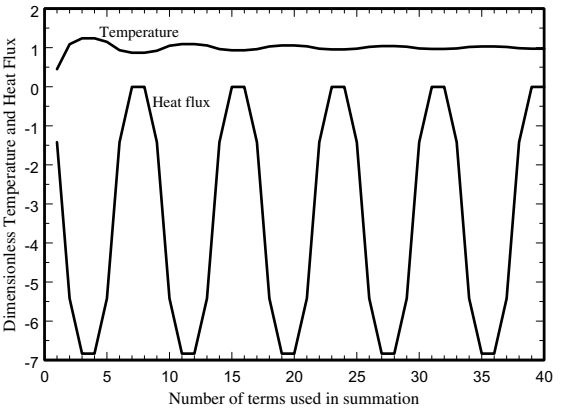

Fig. 2. Dimensionless temperature and heat flux for $x/L = 0.25$, $y/W = 1$, $L_1/L = 0.5$ and $L/W = 1$ using Eqs. (3) and (4).

surface. However, Eq. (7a) does not converge quickly at $x = 0$ and $0 < y < W$ to the correct value of zero while Eq. (3) does.

Accuracy in using Eq. (7b) can be improved by replacing the hyperbolic functions in Eq. (7b) by exponential functions and re-arranging to get

$$A_n\left(\frac{x}{W},\frac{L}{W},\frac{L_1}{W}\right) = \frac{2\mathrm{e}^{-n\pi\frac{x}{W}} + \mathrm{e}^{-n\pi\frac{L_1-x}{W}} - \mathrm{e}^{-n\pi\frac{L_1+x}{W}} + \mathrm{e}^{-n\pi\frac{2L-L_1-x}{W}} - \mathrm{e}^{-n\pi\frac{2L-L_1+x}{W}} - 2\mathrm{e}^{-n\pi\frac{2L-x}{W}}}{2\left(1-\mathrm{e}^{-n\pi\frac{2L}{W}}\right)} \tag{8a}$$

2.2. Solution using non-homogeneous-direction (y-direction) eigenfunctions

The temperature for $0 < x < L_1$ using eigenfunctions in the y-direction is [8–10]

$$T_1(x,y) = T_W\left\{\frac{y}{W} + \sum_{n=1}^{\infty}\frac{2}{n\pi}(-1)^n A_n\left(\frac{x}{W},\frac{L}{W},\frac{L_1}{W}\right) \times \sin\left(n\pi\frac{y}{W}\right)\right\} \tag{7a}$$

$$A_n\left(\frac{x}{W},\frac{L}{W},\frac{L_1}{W}\right) \equiv \left[\sinh\left(n\pi\frac{L-x}{W}\right) + \sinh\left(n\pi\frac{x}{W}\right)\cosh\left(n\pi\frac{L-L_1}{W}\right)\right] \times \left[\sinh\left(n\pi\frac{L}{W}\right)\right]^{-1} \tag{7b}$$

The summation is zero at $y = W$ in Eq. (7a) for $0 < x < L_1$ and the correct temperature is immediately given, unlike Eq. (3) which requires many terms at that

The maximum number of terms required in Eq. (7a) (for the same accuracy as given for Eq. (6)) is

$$n_{\max} = \max\left[\frac{C}{\pi}\frac{W}{x}, \frac{C}{\pi}\frac{W}{L_1-x}\right], \quad C = 23 \tag{8b}$$

This equation is found from the determination of which terms in the numerator of Eq. (8a) have the smallest magnitude exponents as n becomes large. Note that convergence is difficult near $x = 0$ and L_1 for all y-values.

For the region of $L_1 < x < L$, the temperature is given by

$$T_2(x,y) = T_W\sum_{n=1}^{\infty}\frac{2}{n\pi}(-1)^n\frac{1-\cosh\left(n\pi\frac{L_1}{W}\right)}{\sinh\left(n\pi\frac{L}{W}\right)} \times \sinh\left(n\pi\frac{L-x}{W}\right)\sin\left(n\pi\frac{y}{W}\right) \tag{9}$$

Both Eqs. (7a) and (9) give the correct temperature at $y = W$ since $\sin(n\pi) = 0$; this is quite different than the solution given by Eq. (3) but now two equations are required for the $y = W$ surface.

The heat flux in the y-direction in the $0 < x < L_1$ region using Eq. (7a) is

$$q_{y,1}(x,y) = -k\frac{\partial T_1(x,y)}{\partial y} = -\frac{kT_W}{W}\left[1 + 2\sum_{n=1}^{\infty}(-1)^n A_n\left(\frac{x}{W},\frac{L}{W},\frac{L_1}{W}\right) \times \cos\left(n\pi\frac{y}{W}\right)\right] \quad (10a)$$

The heat flux in the y-direction in the region $L_1 < x < L$ using Eq. (9) is

$$q_{y,2}(x,y) = -\frac{kT_W}{W}\sum_{n=1}^{\infty}2(-1)^n\frac{1-\cosh\left(n\pi\frac{L_1}{W}\right)}{\sinh\left(n\pi\frac{L}{W}\right)} \times \sinh\left(n\pi\frac{L-x}{W}\right)\cos\left(n\pi\frac{y}{W}\right) \quad (10b)$$

Provided x is not near either zero or L_1 Eqs. (10a) and (10b) converge quickly at $y = W$, which is in contrast to the oscillatory behavior of Eq. (4) at the $y = W$ surface.

The y-direction heat flux at the $y = W$ surface has interesting characteristics and is much better treated using Eqs. (10a, b) than Eq. (4). For $L_1 = L/2$ and $L = W$, the heat flux values at $y = W$ are given in Table 1; see columns 4 and 5 which display the dimensionless heat flux given by Eq. (10a) for x less than L_1 and Eq. (10b) for the other x-values. Column 4 is for the evaluation of these equations using the hyperbolic functions and column 5 is for the evaluation in terms of the exponential functions. These columns were obtained while using $C = 28$ in Eq. (8b) because 12-digit values are given for some x-values. The heat fluxes are negative for x less than L_1 and positive thereafter. The values start at negative infinity, increase toward zero and then decrease to negative infinity as L_1 is approached. For x just above L_1 the heat fluxes tend to positive infinity and then decrease to zero with increasing x-values. The number of required terms, M, is indicated in the 3rd column. The number of terms is 891 when $x/L = 0.010$ and near the step values of $x/L = 0.490$ and 0.510; even more terms are needed for $0 < x/L < 0.01$ and nearer the step (see the $x/L = 0.499$ row). Column 4, which uses the hyperbolic functions, is both incomplete and inaccurate compared with column 5 (which uses the exponential forms). However, Column 4 has many more accurate components using Eq. (7b) between $x = 0$ and L_1 than a mathematically equivalent form of Eq. (7b) that we previously used. The NaN indicates overflow using Matlab; the italicized digits do not agree with the 5th column which are accurate.

Another surface of interest is at $x = 0$ for the heat flux in the x-direction. The heat flux equation for the y-direction eigenvalues found from Eq. (7a) is

$$q_{x,1}(0,y) = -\frac{kT_W}{W}2\sum_{n=1}^{\infty}(-1)^n\left[-\coth\left(n\pi\frac{L}{W}\right) + \frac{e^{-n\pi\frac{L_1}{W}} + e^{-n\pi\frac{2L-L_1}{W}}}{1-e^{-2n\pi\frac{L}{W}}}\right]\sin\left(n\pi\frac{y}{W}\right) \quad (11)$$

Notice that the exponential function group inside the brackets of this equation goes to zero as n becomes very

Table 1
Steady-state heat flux in the y-direction at $y = W$ using the y-direction eigenfunction

$\frac{x}{L}$	$\frac{L_1}{L}$	M	$\left.\frac{q_y(x,W)}{kT_W/W}\right\|_{\text{hyp}}$	$\left.\frac{q_y(x,W)}{kT_W/W}\right\|_{\text{exp}}$
0.010	0.500	891	NaN	−63.6884042533
0.025	0.500	357	NaN	−25.5309928246
0.050	0.500	178	−12.8657685254	−12.8657685254
0.100	0.500	89	−6.6410002353	−6.6410002353
0.250	0.500	36	−3.4195332875	−3.4195332875
0.400	0.500	89	−4.4611993066	−4.4611993066
0.450	0.500	178	−7.4920012878	−7.4920012878
0.475	0.500	357	NaN	−13.7954636570
0.490	0.500	891	NaN	−32.8599176825
0.499	0.500	8913	NaN	−319.3194693818
0.510	0.500	891	NaN	30.8439702607
0.520	0.500	446	14.9480*063829*	14.9480168813
0.525	0.500	357	11.7743577*183*	11.7743579577
0.550	0.500	178	5.4522878646	5.4522878646
0.750	0.500	36	0.5805225102	0.5805225102
0.950	0.500	20	0.0785206270	0.0785206270
0.975	0.500	19	0.0388287901	0.0388287901
0.990	0.500	18	0.0154836899	0.0154836899

Maximum number of terms with $C = 28$ in Eq. (8b). The fourth column is obtained using the hyperbolic forms, Eq. (7b), and the last column is obtained using the exponential forms, Eq. (8a). M = number terms.

large while the hyperbolic cotangent approaches unity. Consequently the result given by Eq. (11) continues to oscillate with increasing n. For that reason, this equation is not convenient to use whereas Eq. (5) from the x-direction eigenvalue result does converge if $y < W$.

From the above discussion, some conclusions can be made regarding the use of the method of separation of variables for verification purposes for some 2D and 3D steady-state conduction problems. Note that the temperature and the heat flux components may be needed at all surfaces as well as interior points. We conclude that no *one* solution is capable of obtaining the possible T's and q's. In fact, the second formulation itself has two forms, (for $0 < x < L_1$ and $x > L_1$). Second, in some cases special rearrangements are needed such as in going from Eqs. (7b) to (8a). This violates desired Features 2 and 4, listed above. Third, the method has difficulty near the $x = 0$ and $x = L_1$ locations because the number of terms increases rapidly as shown by Table 1, column 3; consequently Feature 5 may not be satisfied.

Another comment is now made regarding the features. When using the separation of variables method for transient heat conduction problems with non-homogeneous boundary conditions, it is common to find the steady-state and transient solutions separately. The transient solution is then usually found by transforming the boundary value problem to an initial value problem which uses the negative of the steady-state solution as the initial condition. If the initial condition has two parts rather than one, more effort is usually needed to derive the transient component of the solution. Moreover, if both solutions are needed, the procedure is further complicated, thus impacting desired Features 2 and 4.

3. Transient time-partitioning method of solution

The heat flux can be accurately and efficiently obtained for the non-homogeneous surface using the transient time-partitioning analysis. Consider a transient version of the above problem with an initial temperature of zero; the number for this case is $X11B00$ $Y11B0(x5)T0$. Using Green's functions the temperature is given by [7, p. 43]

$$T(x,y,t) = \alpha T_W \int_{\tau=0}^{t} \left(-\frac{\partial G_{Y11}}{\partial n'}(y,W,t-\tau) \right) \times \int_{x'=0}^{L_1} G_{X11}(x,x',t-\tau)\,\mathrm{d}x'\,\mathrm{d}\tau \tag{12a}$$

which assumes a step change in temperature at $y = W$ to the constant value of T_W from $x = 0$ to L_1. Notice that the subscripts on the Green's function G are the same as in the case number given above. The n' indicates an outward pointing normal in the y'-direction; it is evaluated at the $y' = W$ surface. The integration on x' is only to L_1 since the boundary temperature is non-zero only from $x' = 0$ to L_1. As in many transient problems, Eq. (12a) involves a convolution; the presentation is simpler, however, if $t - \tau$ (which we shall call the *cotime*) is replaced by u or

$$u \equiv t - \tau \tag{12b}$$

then Eq. (12a) can be written as

$$T(x,y,t) = \alpha T_W \int_{u=0}^{t} \left(-\frac{\partial G_{Y11}}{\partial n'}(y,W,u) \right) \times \int_{x'=0}^{L_1} G_{X11}(x,x',u)\,\mathrm{d}x'\,\mathrm{d}u \tag{12c}$$

In the time-partitioning method, two mathematically equivalent expressions are used for the Green's functions; one is very efficient for "short" values of u while the other is efficient for "long" values of u. The partition cotime t_p between these two regions is sometimes given by [5–7]

$$t_p = 0.05 \min\left(\frac{L^2}{\alpha}, \frac{W^2}{\alpha}\right) = \frac{0.05}{\alpha}\min(L^2, W^2) \tag{13}$$

The two regions are given by

$$\text{short}: \ 0 < u < t_p \quad \text{long}: \ t_p < u < t \tag{14}$$

For the $0 < t < t_p$ interval only the short cotime integral is needed. For the times $t > t_p$, Eq. (12a) is re-written as a short cotime part, $0 < u < t_p$, and a long cotime part, $u > t_p$,

$$\begin{aligned} T(x,y,t) &= \alpha T_W \int_{u=0}^{t_p} \left(-\frac{\partial G^{S}_{Y11}}{\partial n'}(y,W,u) \right) \times \int_{x'=0}^{L_1} G^{S}_{X11}(x,x',u)\,\mathrm{d}x'\,\mathrm{d}u + \alpha T_W \\ &\quad \times \int_{u=t_p}^{t} \left(-\frac{\partial G^{L}_{Y11}}{\partial n'}(y,W,u) \right) \times \int_{x'=0}^{L_1} G^{L}_{X11}(x,x',u)\,\mathrm{d}x'\,\mathrm{d}u \\ &= T^{S}(x,y,t_p) + T^{L}(x,y,t_p,t) \end{aligned} \tag{15}$$

3.1. Short cotime form

The derivative and the integral of the Green's function are needed in Eq. (15) both for the short and long cotime forms, $T^{S}(x,y,t_p)$ and $T^{L}(x,y,t_p,t)$. Approximate short cotime forms for the Green's function needed above are [7, p. 481, 482]

$$G^{S}_{X11}(x,x',u) \approx \frac{1}{\sqrt{4\pi\alpha u}} \left[\mathrm{e}^{-\frac{(x-x')^2}{4\alpha u}} - \mathrm{e}^{-\frac{(x+x')^2}{4\alpha u}} - \mathrm{e}^{-\frac{(2L-x-x')^2}{4\alpha u}} + \mathrm{e}^{-\frac{(2L-x+x')^2}{4\alpha u}} \right] \tag{16a}$$

$$-\frac{\partial G^{\mathrm{S}}_{Y11}}{\partial n'}(y,W,u)\approx\frac{W-y}{\sqrt{4\pi[\alpha u]^3}}\mathrm{e}^{-\frac{(W-y)^2}{4\alpha u}}-\frac{W+y}{\sqrt{4\pi[\alpha u]^3}}\mathrm{e}^{-\frac{(W+y)^2}{4\alpha u}} \tag{16b}$$

$$\int_{x'=0}^{L_1}G^{\mathrm{S}}_{X11}(x,x',u)\,\mathrm{d}x'\approx\frac{1}{2}\sum_{i=1}^{6}B_i\,\mathrm{erfc}\left(\frac{w_i}{\sqrt{4\alpha u}}\right) \tag{17}$$

where

$$B_1=-2,\quad B_2=B_3=1,\quad B_4=2,\quad B_5=B_6=-1 \tag{18}$$

$$w_1=x,\quad w_2=x-L_1,\quad w_3=x+L_1,\quad w_4=2L-x,\quad w_5=2L-x-L_1,\quad w_6=2L-x+L_1 \tag{19}$$

Eqs. (16)–(18) are very accurate for $\alpha u/L^2$ less than 0.05 for $W=L$. For points near or at the non-homogeneous surface of $y=W$, only the first term on the right of Eq. (16b) provides sufficient accuracy as demonstrated below; in that case, the problem is modeled as a semi-infinite body and is denoted $Y01$ rather than $Y11$.

Using the first term in Eq. (16b) and (17) in Eq. (15) gives the short cotime temperature expression,

$$\begin{aligned}T^{\mathrm{S}}(x,y,t_{\mathrm{p}})&\approx\alpha T_W\int_{u=0}^{t_{\mathrm{p}}}\frac{W-y}{\sqrt{4\pi[\alpha u]^3}}\mathrm{e}^{-\frac{(W-y)^2}{4\alpha u}}\\&\quad\times\frac{1}{2}\sum_{i=1}^{6}B_i\,\mathrm{erfc}\left(\frac{w_i}{\sqrt{4\alpha u}}\right)\mathrm{d}u\\&=T_W\frac{1}{\sqrt{\pi}}\sum_{i=1}^{6}B_i\frac{W-y}{\sqrt{4\alpha}}I_5\left(\frac{W-y}{\sqrt{4\alpha}},\frac{w_i}{\sqrt{4\alpha}},\frac{1}{\sqrt{t_{\mathrm{p}}}}\right)\end{aligned} \tag{20}$$

$$I_5(a,b,\Theta)\equiv\frac{1}{2}\int_{u=0}^{\Theta^{-2}}\frac{1}{u^{3/2}}\mathrm{e}^{-\frac{a^2}{u}}\mathrm{erfc}\left(\frac{b}{\sqrt{u}}\right)\mathrm{d}u,\quad\Theta=\frac{1}{\sqrt{t}} \tag{21}$$

The I_5-function is treated in Appendix A. At $y=W$, the values given by Eq. (20) for $x>L_1$ are zero; for $0<x<L_1$ the use of Eq. (A.4) gives the correct result of T_W. A significant difference between the above analysis and that in [5] is that the integral in Eq. (20) is evaluated exactly rather than using numerical integration. We note that Eq. (20) is evaluated with a known truncation error rather than a quadrature which often uses a heuristic termination.

3.2. Long cotime form

The long cotime forms analogous to Eqs. (16a,b) and (17) are [4, p. 482, 483]

$$G^{\mathrm{L}}_{X11}(x,x',u)=\frac{2}{L}\sum_{m=1}^{\infty}\mathrm{e}^{-(m\pi)^2\frac{\alpha u}{L^2}}\sin\left(m\pi\frac{x}{L}\right)\sin\left(m\pi\frac{x'}{L}\right) \tag{22a}$$

$$-\frac{\partial G^{\mathrm{L}}_{Y11}}{\partial n'}(y,W,u)=-\frac{2\pi}{W^2}\sum_{n=1}^{\infty}\mathrm{e}^{-(n\pi)^2\frac{\alpha u}{W^2}}n(-1)^n\sin\left(n\pi\frac{y}{W}\right) \tag{22b}$$

$$\int_{x'=0}^{L_1}G^{\mathrm{L}}_{X11}(x,x',u)\,\mathrm{d}x'=\frac{2}{\pi}\sum_{m=1}^{\infty}\mathrm{e}^{-(m\pi)^2\frac{\alpha u}{L^2}}\frac{1}{m}\sin\left(m\pi\frac{x}{L}\right)\times\left[1-\cos\left(m\pi\frac{L_1}{L}\right)\right] \tag{23}$$

Though these equations are exact for all times, they are used here only for long cotimes, to take advantage of their convergence properties.

Introducing Eqs. (22b) and (23) into the $T^{\mathrm{L}}(x,y,t_{\mathrm{p}},t)$ portion of Eq. (15) gives

$$T^{\mathrm{L}}(x,y,t_{\mathrm{p}},t)=-\frac{4\alpha T_W}{W^2}\int_{u=t_{\mathrm{p}}}^{t}\sum_{m=1}^{\infty}\sum_{n=1}^{\infty}\mathrm{e}^{-\lambda_{mn}^2\pi^2\frac{\alpha u}{W^2}}\times\Phi_{mn}(x,y,L,W,L_1)\,\mathrm{d}u \tag{24}$$

where

$$\lambda_{mn}^2\equiv\left(m\frac{W}{L}\right)^2+n^2 \tag{25a}$$

$$\Phi_{mn}(x,y,L,W,L_1)=\frac{n(-1)^n}{m}\sin\left(n\pi\frac{y}{W}\right)\sin\left(m\pi\frac{x}{L}\right)\times\left[1-\cos\left(m\pi\frac{L_1}{L}\right)\right] \tag{25b}$$

We define the "complementary transient temperature" (see subscript c.t.) as

$$T^{\mathrm{L}}_{\mathrm{c.t.}}(x,y,u)=\frac{4T_W}{\pi^2}\sum_{m=1}^{\infty}\sum_{n=1}^{\infty}\frac{1}{\lambda_{mn}^2}\mathrm{e}^{-\lambda_{mn}^2\pi^2\frac{\alpha u}{W^2}}\times\Phi_{mn}(x,y,L,W,L_1) \tag{26}$$

Then Eq. (24) can be written as

$$T^{\mathrm{L}}(x,y,t_{\mathrm{p}},t)=T^{\mathrm{L}}_{\mathrm{c.t.}}(x,y,t)-T^{\mathrm{L}}_{\mathrm{c.t.}}(x,y,t_{\mathrm{p}}) \tag{27}$$

Using the same criterion used in Eq. (6), the number of terms can be found by restricting exponents in Eq. (26) so that

$$\left[\left(m\frac{W}{L}\right)^2+n^2\right]\pi^2\frac{\alpha u}{W^2}=\left(\frac{m}{L/(\pi\sqrt{\alpha u})}\right)^2+\left(\frac{n}{W/(\pi\sqrt{\alpha u})}\right)^2\leqslant C=23 \tag{28}$$

The accuracy constant C can be 23 and other values as shown below. Using Eq. (28), the total number of terms in the summation in Eq. (26) can be estimated by computing 1/4 of the area of the ellipse in terms of m and n; the area is the product of the semi-axes multiplied by π. This then gives the approximate number of terms as

$$\#\text{ terms}\approx\frac{C}{4\pi}\frac{LW}{\alpha u}=\frac{23}{4\pi}\frac{LW}{\alpha u} \tag{29}$$

Hence the number of terms increases linearly with L, W and C but decreases with increasing cotime u. Consequently, for a given geometry the number of terms is decreased when the partition cotime t_p is maximized.

A general equation for the temperature in terms of the short cotime part and the complementary transient terms is now given. Using Eq. (27) in the second part of Eq. (15) gives the temperature for $t > t_p$ as

$$T(x,y,t) = T^S(x,y,t_p) + T^L(x,y,t_p,t) = T^S(x,y,t_p) + T^L_{c.t.}(x,y,t) - T^L_{c.t.}(x,y,t_p) \quad (30)$$

The y-direction heat flux component found from Eq. (30) is

$$q_y(x,y,t) = q_y^S(x,y,t_p) + q^L_{y,c.t.}(x,y,t) - q^L_{y,c.t.}(x,y,t_p) \quad (31)$$

Internal verification of time-partitioning solutions uses Eqs. (30) and (31) with two or more appropriate partition times; the calculated temperature (and heat fluxes) should be very nearly the same for each of these partition times. We call this the "partition-time verification test." See the discussion in connection with Table 2.

4. Steady state from the time-partition method

The steady-state temperature can be obtained from Eq. (30) by letting the time t go to infinity which causes the $T^L_{c.t.}(x,y,\infty)$ term to go to zero (see Eq. (26)); hence

$$T(x,y,\infty) = T^S(x,y,t_p) - T^L_{c.t.}(x,y,t_p) \quad (32a)$$

In words, this equation states that the steady state for this problem is the short cotime temperature minus the complementary transient temperatures, both evaluated at the same partition cotime. Similarly for the steady-state heat flux, we can write

$$q_y(x,y,\infty) = q_y^S(x,y,t_p) - q^L_{c.t.,y}(x,y,t_p) \quad (32b)$$

Using this relation provides insight into the time-partitioning computational process. For example, the "same" answer should be obtained as the partition cotime is changed. Recall that the two components of Eq. (32b) are independent but yet the sum should be the same. The difference in any values of the heat flux as the partition cotime is decreased is a measure of the error. These points are illustrated below.

The heat flux in the y-direction is found from Eqs. (20) and (24) for the short and long cotime components, respectively. Using Eq. (20) and Eq. (A.5a), the short cotime component of the heat flux is

$$q_y^S(x,y,t_p) \approx \frac{kT_W}{\sqrt{4\pi\alpha t_p}} e^{-\frac{(W-y)^2}{4\alpha t_p}} \times \sum_{i=1}^{6} B_i \left[\frac{2w_i\sqrt{\alpha t_p/\pi}}{(W-y)^2 + w_i^2} e^{-\frac{w_i^2}{4\alpha t_p}} - \operatorname{erfc}\left(\frac{w_i}{\sqrt{4\alpha t_p}}\right)\right] \quad (33)$$

which is valid for *all* x- values in $0 < x < L$. Evaluating this equation at $y = W$ gives

Table 2
Steady-state heat fluxes using Eq. (37) for the point $x = L/4$ and $y = W$ for the case of $T = T_W$ from $x = 0$ to $L_1 = L/2$ at the $y = W$ surface and other surfaces at $T = 0$, $W/L = 1$

$\frac{\alpha t_p}{W^2}$	$\frac{x}{L}$	C	M	$\frac{q_y^S(x,W,t_p)}{kT_W/L}$	$\frac{q^L_{y,ct}(x,W,t_p)}{kT_W/L}$	$\frac{q_y(x,W,t_\infty)}{kT_W/L}$
0.030	0.25	20	45	−4.0239024278	−0.6043691382	−3.4195332*896*
0.080	0.25	20	15	−3.5326417253	−0.1131115982	−3.4195*301271*
0.020	0.25	23	81	−4.4737502048	−1.0542169174	−3.4195332875
0.030	0.25	23	52	−4.0239024278	−0.6043691403	−3.4195332875
0.040	0.25	23	39	−3.8099530542	−0.3904197668	−3.4195332*874*
0.050	0.25	23	30	−3.6901784372	−0.2706451525	−3.4195332*847*
0.060	0.25	23	24	−3.6160491458	−0.1965159269	−3.4195332*190*
0.080	0.25	23	19	−3.5326417253	−0.1131115993	−3.4195*301260*
0.250	0.250	23	4	−3.4209184949	−0.0032417630	−3.4*176767320*
0.030	0.250	26	60	−4.0239024278	−0.6043691404	−3.4195332875
0.080	0.250	26	20	−3.5326417253	−0.1131115993	−3.4195*301260*
0.030	0.49	23	52	−33.5138048380	−0.6538871555	−32.8599176*826*
0.040	0.49	23	39	−33.3163537525	−0.4564360700	−32.8599176825
0.050	0.49	23	30	−33.1935997314	−0.3336820530	−32.8599176*784*
0.080	0.49	23	19	−33.0115253050	−0.1516121776	−32.8599*31275*
0.030	0.499	26	60	−319.9657792055	−0.6463098235	−319.3194693*821*
0.080	0.499	26	20	−319.4708064789	−0.1513416278	−319.3194*648511*

$$q_y^{\mathrm{S}}(x,W,t_{\mathrm{p}}) = -k\frac{\partial T^{\mathrm{S}}(x,W,t_{\mathrm{p}})}{\partial y} \approx \frac{kT_W}{\sqrt{\pi}}\sum_{i=1}^{6}\frac{B_i}{w_i}\mathrm{ierfc}\left(\frac{w_i}{\sqrt{4\alpha t_{\mathrm{p}}}}\right) \tag{34}$$

For the ierfc function, see Eq. (A.2b). For the region $0 < x < L_1$, it is convenient to use the relation

$$\frac{1}{\sqrt{\pi}(L_1-x)}\mathrm{ierfc}\left(\frac{x-L_1}{\sqrt{4\alpha t_{\mathrm{p}}}}\right) = \frac{1}{\sqrt{\pi}(L_1-x)}\mathrm{ierfc}\left(\frac{L_1-x}{\sqrt{4\alpha t_{\mathrm{p}}}}\right) + \frac{1}{\sqrt{\pi\alpha t_{\mathrm{p}}}}$$

Using this result and expanding Eq. (34) gives

$$\begin{aligned} q_y^{\mathrm{S}}(x,W,t_{\mathrm{p}}) \approx kT_w\Bigg\{ & -\frac{1}{\sqrt{\pi\alpha t_{\mathrm{p}}}} - \frac{2}{x\sqrt{\pi}}\mathrm{ierfc}\left(\frac{x}{\sqrt{4\alpha t_{\mathrm{p}}}}\right) \\ & - \frac{1}{(L_1-x)\sqrt{\pi}}\mathrm{ierfc}\left(\frac{L_1-x}{\sqrt{4\alpha t_{\mathrm{p}}}}\right) + \frac{1}{(L_1+x)\sqrt{\pi}}\mathrm{ierfc}\left(\frac{L_1+x}{\sqrt{4\alpha t_{\mathrm{p}}}}\right) + \frac{2}{(2L-x)\sqrt{\pi}}\mathrm{ierfc}\left(\frac{2L-x}{\sqrt{4\alpha t_{\mathrm{p}}}}\right) \\ & - \frac{1}{(2L-x-L_1)\sqrt{\pi}}\mathrm{ierfc}\left(\frac{2L-x-L_1}{\sqrt{4\alpha t_{\mathrm{p}}}}\right) - \frac{1}{(2L-x+L_1)\sqrt{\pi}}\mathrm{ierfc}\left(\frac{2L-x+L_1}{\sqrt{4\alpha t_{\mathrm{p}}}}\right)\Bigg\} \end{aligned} \tag{35}$$

The various terms in Eq. (35) can be associated with the treatment of different boundary conditions; four different conditions can be described. (1) The term, *term* $1 = -1/\sqrt{\pi\alpha t_{\mathrm{p}}}$, is for a 1D semi-infinite body with a constant surface temperature; it is denoted $Y01BT0$. (2) *term* 1 plus *term* $2(= -[2/(x\sqrt{\pi})]\mathrm{ierfc}(x/\sqrt{4\alpha t_{\mathrm{p}}}))$ is for the quarter-infinite region with $T = T_W$ at $y = W$ and $T = 0$ at $x = 0$; the number is $X10B0\ Y01B1T0$. Parenthetically we note that *term* 2 divided by $-1/\sqrt{\pi\alpha t_{\mathrm{p}}}$ is less than $1.0E-10$ for the Fourier number $\alpha t_{\mathrm{p}}/x^2$ less than 0.014. Consequently for $x < L_1/2$ and this Fourier number less than 0.014, only the $Y01BT0$ model in needed for this problem. (3) Adding the two terms with $L_1 - x$ and $L_1 + x$ includes the effect of the finite isothermal surface temperature of T_W ending at L_1; this problem is denoted $X10B0\ Y01B(x5)T0$. (4) Adding the final three terms in the summation of Eq. (35) treats the finite boundary at $x = L$; the number is $X11B0\ Y01B(x5)T0$. Another aspect is that Eq. (35) gives negative infinite heat flux values both as x goes to zero and also as x approaches L_1 from below. As x approaches L_1 above, the heat flux values go to positive infinity.

Now the long cotime component heat flux of Eq. (32b) is needed. Using Eq. (26), the complementary transient y-direction heat flux is

$$q_{\mathrm{c.t.},y}^{\mathrm{L}}(x,y,u) = -k\frac{4T_W}{\pi^2}\sum_{m=1}^{\infty}\sum_{n=1}^{\infty}\frac{1}{\lambda_{mn}^2}\mathrm{e}^{-\lambda_{mn}^2\pi^2\frac{\alpha u}{W^2}} \times \frac{\partial\Phi_{mn}(x,y,L,W,L_1)}{\partial y} \tag{36a}$$

$$\frac{\partial\Phi_{mn}(x,y,L,W,L_1)}{\partial y} = \frac{n^2\pi(-1)^n}{mW}\cos\left(n\pi\frac{y}{W}\right)\sin\left(m\pi\frac{x}{L}\right) \times \left[1-\cos\left(m\pi\frac{L_1}{L}\right)\right] \tag{36b}$$

Using Eqs. (35) and (36a) in Eq. (32b), the steady-state heat flux in the y-direction at $y = W$ is

$$\begin{aligned} & q_y(x,W,\infty) \\ & = -k\frac{\partial T}{\partial y}(x,W,\infty) = q_y^{\mathrm{S}}(x,W,t_{\mathrm{p}}) - q_{\mathrm{c.t.},y}^{\mathrm{L}}(x,W,t_{\mathrm{p}}) \\ & = kT_W\Bigg\{ -\frac{1}{\sqrt{\pi\alpha t_{\mathrm{p}}}} + \Bigg[-\frac{2}{x\sqrt{\pi}}\mathrm{ierfc}\left(\frac{x}{\sqrt{4\alpha t_{\mathrm{p}}}}\right) - \frac{1}{(L_1-x)\sqrt{\pi}}\mathrm{ierfc}\left(\frac{L_1-x}{\sqrt{4\alpha t_{\mathrm{p}}}}\right) + \frac{1}{(L_1+x)\sqrt{\pi}}\mathrm{ierfc}\left(\frac{L_1+x}{\sqrt{4\alpha t_{\mathrm{p}}}}\right) \\ & \quad + \sum_{i=4}^{6}\frac{B_i}{w_i\sqrt{\pi}}\mathrm{ierfc}\left(\frac{w_i}{\sqrt{4\alpha t_{\mathrm{p}}}}\right)\Bigg]\Bigg\} + \frac{4kT_W}{\pi^2}\sum_{m=1}^{\infty}\sum_{n=1}^{\infty}\frac{1}{\lambda_{mn}^2} \times \exp\left(-\lambda_{mn}^2\pi^2\frac{\alpha t_{\mathrm{p}}}{W^2}\right)\frac{\partial\Phi_{mn}(x,W,L,W,L_1)}{\partial y} \end{aligned} \tag{37}$$

which is valid for all x's on the $y = W$ surface, not just for $0 < x < L_1$. By choosing a sufficiently small partition time and the appropriate number of terms, 10 or more digit accuracy can be achieved, as is demonstrated below. For the transient heat flux, the complementary transient term given by Eq. (36a) for $u = t$ is simply added to Eq. (37) (see Eq. (31)).

4.1. Example of calculation of heat flux at $y = W$

Calculation of the steady-state heat flux for $x/L = 0.25$, $y/W = 1$, $L_1/L = 0.5$ and $L/W = 1$ is now treated using Eq. (37). The problem can be solved using the four different short cotime models, each of which is discussed below Eq. (35). With each using its own appropriate dimensionless partition cotime, the answers to this problem for each model agree to about 10 significant figures. However, the number of required terms for a simplified model is greater than a more complete one. Below, the main attention is given the short cotime model which explicitly considers all the boundary conditions except that at $y = 0$. More precisely, Eq. (37) is used with all the terms in the summation.

Table 2 displays numerical values for this model and dimensionless partition cotimes from 0.02 to 0.25. Also, the three values of the accuracy constant C equal to 20,

23 and 26 are displayed for $x/L = 0.25$. Abbreviated results are also given for $x/L = 0.49$ and 0.499. Columns 5, 6 and 7 in Table 2 give the short cotime component, the complementary transient component and the steady-state heat flux, respectively. The last of these is obtained by subtracting Column 6 from Column 5, as indicated by Eq. (32b).

Table 2 illustrates the two accuracy-related criteria utilized in the time-partitioning method. The two criteria are values of the dimensionless partition cotime, $\alpha t_p/W^2$, and of the C exponent, Eq. (28). The partition cotime is dependent upon the short cotime expression, Eq. (35); as the partition cotime is decreased, greater accuracy in the short cotime of the solution is obtained but more terms are needed in the long cotime component of the solution. The C exponent is related to the error in the long cotime expression, Eq. (36); as it is made larger, greater accuracy in the long cotime numerical value is obtained and again the number of terms is increased. The number of terms in the short cotime part is fixed because the long cotime part is easier to manipulate and the number of terms is easily adjusted. Provided the dimensionless partition cotime is small enough and C is large enough, the numerical values of steady-state heat flux are accurate to the number of digits given; notice that the $C = 23$ and 26 value for the smallest dimensionless partition cotimes agree with the one for $x/L = 0.25$ in Table 1; namely, −3.4195332875.

The dimensionless cotime is ideally chosen to be the largest possible to get the desired accuracy. Since the $Y01$ approximation is used for the $y = W$ surface, the second term of Eq. (16b) is dropped in the above short cotime analysis because it is not needed for $\alpha t_p/W^2 \leqslant 0.05$. This is confirmed by the $C = 23$ values for $x/L = 0.25$ in Table 2; nine significant figure accuracy is given by the $\alpha u/W^2 = 0.05$ value (the italicized digits are inaccurate). For the smaller dimensionless cotime of 0.04, there is 10 digit accuracy and for even smaller cotimes, accuracy to 11 digits is given in Table 2 for $C = 23$. Decreasing C to 20 gives less slightly less accuracy (to 9 digits) as shown in Table 2 even when the small partition cotime of 0.03 is used. On the other hand for the $x/L = 0.25$ location and $C = 26$, no changes in the final answers are given compared to the $C = 23$ computations.

Table 2 also displays results for $x/L = 0.49$ and 0.499. The numerical values agree very closely with those in Table 1. The values for $x/L = 0.499$ agree to 11 digits and agree to 12 if rounded. In this case, the time-partitioning solution given in Table 2 for $\alpha u/W^2 = 0.03$ needs 60 terms while the steady-state solution displayed in Table 1 needs 8913 terms. As the critical locations of $x = 0$ or $x = L_1$ at $y = W$ are approached, the steady-state solution in Table 1 requires many more terms than away from these locations. In contrast, the number of terms in the time-partitioning solution in Table 2 is independent of these locations for the same value of C; only 60 terms are needed for the $C = 26$ value and $\alpha u/W^2 = 0.03$ (60 terms is less than 1% of the 8913 number of terms found using the steady-state solution). Notice that the short cotime contribution is about −319.96 while the long cotime portion is about −0.646 so the long cotime contribution is relatively small in this case. This is clearly not a close subtraction of numerical values.

Closer subtractions of values occur when the simple semi-infinite model is used. The model is the first one given below Eq. (35) and is $-1/\sqrt{\pi\alpha t_p}$ and has the notation of $Y01BT0$. A small dimensionless partition cotime is needed, such as 0.0005. For the location of $x/L = 0.25$ and $C = 26$, the 5th and 6th columns corresponding to Table 2 are −25.2313252202 and −21.8117919327; subtracting the 2nd term from the 1st term gives the same result as previously obtained of −3.4195332875. The subtraction did not degrade the answer in this case. This solution required 4069 terms and more would be required as the x-location moves closer to the critical locations of $x = 0$ or L_1. The potentially large number of terms is a disadvantage of using this simple model ($Y01BT0$.)

A unique and powerful feature of the time-partitioning method is the internal verification of the solution. Another is predicting the accuracy of the solution. The internal verification principle is that the computed temperature and heat fluxes should go to constant values as the partition cotime decreases. These constant values should be the correct values to as many decimal places as indicated. Provided the C-value is sufficiently large, that is exactly what is demonstrated in Table 2. For example, for $C = 23$ and $x/L = 0.25$, reducing the dimensionless partition cotime has the effect of the numerical values approaching the accurate value of −3.4195332875. We note that the two numerical components of the solution (5th and 6th columns) are completely independent. The short cotime and the long cotime parts have entirely different mathematical forms and have no common computations. In fact, the two parts of the solution given by Eq. (37) have two physical interpretations; the short cotime is for a body semi-infinite in the y-direction and is denoted $X11B00$ $Y01B(x5)0T0$ while the long-cotime part treats the $y = 0$ boundary condition and is denoted $X11B00$ $Y11B(x5)0T0$. In our work, this internal verification of solutions has been repeatedly used and it has been very helpful and powerful [5,6].

Consider now the point of predicting the accuracy. Notice for $C = 23$ and $x/L = 0.25$ results of Table 2 that numerical values monotonically improve as the partition cotimes decrease. The heat flux values for partition cotimes of 0.06 and 0.08 are −3.4195332190 and −3.4195301260, respectively. Since they agree with the value of −3.41953, this value is expected to be correct to

these six digits. This gives an estimate of the accuracy of the 0.08 partition-time answer. When the values do not change in the digits displayed, the values should be accurate to these digits.

5. Transient cases

The time-partitioning method provides transient heat conduction solutions in a very similar manner as the steady state is calculated. Table 2, for example, can be used to obtain transient y-direction heat fluxes for the point $x = L/4$ and $y = W$ for the case denoted $X11B00$ $Y11B0(x5)T0$ with the unity aspect ratio. Consider the y-direction heat flux. Combining Eqs. (31) and (32a) gives

$$q_y(x,y,t) = q^{\mathrm{L}}_{y,\mathrm{c.t.}}(x,y,t) + q_y(x,y,\infty) \tag{38}$$

which states that the heat flux at a particular location and time is equal to the complementary component evaluated at the same location and time plus the steady-state value. A similar equation can be written for the x-direction heat flux and the temperature. For the point mentioned above, we know the value of the y-direction steady-state heat flux, namely, -3.4195332875 in dimensionless form. For the dimensionless time of 0.25, this y-direction heat flux is $-0.0032417630 + (-3.4195332875) = -3.4227750505$ in dimensionless form. Other values can be found in a similar way.

The usage of the words "complementary transient" for the first term in Eq. (38) is relatively recent but an analogous equation is given by Eq. (3.61) of Ref. [7, p. 56]. ("Analogous" is used because T is used in [7] instead of q.) If the alternative Green's function solution equation in [7] is restricted to time-invariant boundary conditions, the complementary transient term in Eq. (38) is analogous to the T' term of Eq. (3.61) and the steady-state term in Eq. (38) is analogous to the T^* term.

6. Comments on features of the time-partitioning solution

The time-partitioning solution for verification satisfies most if not all of the desired features given at the beginning of this paper. These comments are now reviewed. Feature 1 is regarding extreme accuracy for the temperature and the heat fluxes; this is demonstrated above. Feature 2 relates to large improvements in accuracy without excessive computational cost or change in procedure. This is also demonstrated; we note that using Eq. (29) with the exponent criterion C of 11.5 gives errors about $1.0\mathrm{E}-5$ and with $C = 23$ the errors are about $1.0\mathrm{E}-10$. Then the errors are reduced by about a factor of $1.0\mathrm{E}-5$ while the number of terms in the double series only increases by about a factor of 2. For Feature 3, the only finite boundary condition treated in this paper is the first kind, prescribed temperature. The basic method has been demonstrated for the other boundary conditions of the 2nd and 3rd kinds in [5] but integration over the dummy cotime is required. The present paper uses an exact integral in the solution. Some of the required integrals are difficult to obtain but a number have been obtained by Amos [11] in connection with this research. Feature 4 is about using the same basic 1D building blocks for the 1D, 2D and 3D cases. That is satisfied because they can be used in a multiplicative manner for homogeneous plates, rectangles and parallelepipeds; it is not true for the usual steady-state solutions using separation of variables. Features 5 and 6 regarding corners and small times are shown herein to be satisfied. Feature 7, extension to other coordinates, is not demonstrated but is satisfied particularly for cylindrical coordinates. Extension to solid body flow [3,4] has been demonstrated elsewhere. The two bonus features of internal verification and indication of accuracy are also shown in connection with Table 2.

7. Summary and conclusions

Solutions using separation of variables for steady-state heat conduction problems in multi-dimensional heat conduction can require more than one form of the solution, particularly at the boundaries. These solutions may be completely satisfactory, particularly if only the steady state is needed [9,10]. However, for obtaining robust solutions for verification with transient solutions also of interest, the time-partitioning method offers some advantages. As mentioned, more than one form of the solution may be needed using the steady-state separation of variables method; two basic forms for 2D problems and three forms for 3D problems are needed. Even after obtaining the solutions, special treatment of the hyperbolic terms may be necessary. The time-partitioning method does not have these problems. Near corners and near discontinuous boundary temperatures, even the most appropriate steady-state solution may require a very large number of terms and the solution may not clearly indicate that the heat flux goes to infinity. Again the time-partitioning method is demonstrated herein to very effectively treat these conditions for the problem treated.

The time-partitioning method satisfies most if not all of the desired features for verification cited at the beginning of this paper. The same method provides transient and steady-state values for the temperature and the heat flux components. It is not necessary to have multiple forms of the steady-state solution. No special re-arrangement of hyperbolic terms is needed to obtain a solution. Special integrals [11] have been developed to aid in evaluating the integrals over the dummy cotime variable. Powerful and unique features of the time-partitioning method are the bonus features of internal verification and accuracy indication.

Acknowledgements

The support of this research by Sandia National Laboratories, Albuquerque, NM is appreciated. Dr. Kevin Dowding was the Project Manager at Sandia. Suggestions by Dr. Arafa Osman are appreciated.

Appendix A. I_5-function

The I_5-function is (Amos, Folder 5, [11])

$$I_5(a,b,\Theta) \equiv \frac{1}{2}\int_{u=0}^{\Theta^{-2}} \frac{1}{u^{3/2}} \mathrm{e}^{-\frac{a^2}{u}} \mathrm{erfc}\left(\frac{b}{\sqrt{u}}\right) \mathrm{d}u = \int_{\Theta}^{\infty} \mathrm{e}^{-a^2w^2} \mathrm{erfc}(bw)\,\mathrm{d}w, \Theta = \frac{1}{\sqrt{t}} \tag{A.1}$$

Both $\exp(-a^2w^2)$ and $\mathrm{erfc}(bw)$ are less than unity for $a > 0$ and $b > 0$ and decrease rapidly with increasing w. For either $a^2\Theta^2$ or $b^2\Theta^2 \geqslant 23$, the I_5-function is nearly equal to zero since $\exp(-23) \approx 1.0\mathrm{E}-10$ and $\mathrm{erfc}(\sqrt{23}) \approx 1.0\mathrm{E}-11$. An infinite series for $a \leqslant b$ is given by

$$I_5(a,b,\Theta) = \frac{1}{2d\sqrt{\pi}} \sum_{k=0}^{\infty} C_k \left(\frac{a^2}{d^2}\right)^k E_{k+3/2}(d^2\Theta^2), \quad d = \sqrt{a^2+b^2}$$
$$C_0 = 1, \quad C_k = \frac{(1/2)_k}{k!} = \frac{1}{k!}\prod_{j=0}^{k-1}\left(\frac{1}{2}+j\right) \quad \text{for } k = 1,2,3,\ldots \tag{A.2a}$$

Some programs such as Mathematica give the exponential integral for different values of k. For other programs, a recursion relation for the exponential integral function is [12,13]

$$E_{k+3/2}(d^2\Theta^2) = \frac{2}{2k+1}\left[\mathrm{e}^{-d^2\Theta^2} - d^2\Theta^2 E_{k+1/2}(d^2\Theta^2)\right]$$
$$E_{3/2}(d^2\Theta^2) = 2\sqrt{\pi}\,\mathrm{ierfc}(d\Theta), \quad \mathrm{ierfc}(z) = \pi^{-1/2}\mathrm{e}^{-z^2} - z\,\mathrm{erfc}(z) \tag{A.2b}$$

However, this recursion relation must be used with care. This recurrence is not stable when the recurrence is carried forward to an index k close to $d^2\Theta^2$. Thus, when $d^2\Theta^2$ is large, the first part of the sequence generates error. The correct way is to start the recurrence where the value near the integer part of $d^2\Theta^2$ is generated and recurrence is carried up and down from this index. See Example 6 at the end of Chapter 5 of Ref. [14].

The C_k and exponential integral in Eq. (A.2a) decrease slowly with k but the $(a^2/d^2)^k$ term decreases much more rapidly. For $a \leqslant b$, the ratio a^2/d^2 is less than or equal to 1/2. Setting this term equal to 10^{-10} and solving for the maximum value of k gives $k_{\max} = 10/\log[1+(b/a)^2]$. If $b = a$, about 33 terms are needed but if $b = 3a$, only 10 terms are needed.

For $a > b$, use [11, p. 5.7]

$$I_5(a,b,\Theta) = \frac{\sqrt{\pi}}{2a}\mathrm{erfc}(a\Theta)\,\mathrm{erfc}(b\Theta) - \frac{b}{a}I_5(b,a,\Theta) \tag{A.3}$$

For $a = b$, this equation gives $I_5(a,a,\Theta) = (\sqrt{\pi}/4a) \times \mathrm{erfc}^2(a\Theta)$. For negative values of b, use

$$I_5(a,b,\Theta) = \frac{\sqrt{\pi}}{a}\mathrm{erfc}(a\Theta) - I_5(a,-b,\Theta) \tag{A.4}$$

If $b < 0$ and $b^2\Theta^2 > 23$, then the I_5-function on the right side of Eq. (A.4) disappears.

It can be shown that the derivative of $aI_5(a,b,\Theta)$ with respect to a is

$$\frac{\partial[aI_5(a,b,\Theta)]}{\partial a} = \mathrm{e}^{-a^2\Theta^2}\left[\frac{b}{(a^2+b^2)\sqrt{\pi}}\mathrm{e}^{-b^2\Theta^2} - \Theta\mathrm{erfc}(b\Theta)\right] \tag{A.5a}$$

If a is equal to zero, Eq. (A.5a) gives (see Eq. (A.2b) for ierfc(·))

$$\left.\frac{\partial[aI_5(a,b,\Theta)]}{\partial a}\right|_{a=0} = \frac{1}{b\sqrt{\pi}}\mathrm{e}^{-b^2\Theta^2} - \frac{b\Theta}{b}\mathrm{erfc}(b\Theta) = \frac{1}{b}\mathrm{ierfc}(b\Theta) \tag{A.5b}$$

The derivative of $I_5(a,b,\Theta)$ with respect to b is

$$\frac{\partial I_5(a,b,\Theta)}{\partial b} = \frac{-1}{(a^2+b^2)\sqrt{\pi}}\mathrm{e}^{-(a^2+b^2)}\Theta^2 \tag{A.6}$$

Appendix B. Bounds for $I_5(a,b,)$ for $a>0$, $b>0$ and $\Theta \geqslant 0$

Integral $I_5(a,b,\Theta)$ exists if a or b is equal to zero, but not both at the same time. One bound is

$$I_5(a,b,\Theta) \leqslant I_5(a,b,0) = \frac{1}{a\sqrt{\pi}}\tan^{-1}\left(\frac{a}{b}\right) \tag{B.1}$$

A better bound is found using Mill's ratio (Ref. [14, p. 298, Eq. (7.1.13)]),

$$\mathrm{erfc}(x) \leqslant \frac{2}{\sqrt{\pi}}\frac{\mathrm{e}^{-x^2}}{x+\sqrt{x^2+4/\pi}}, \quad x \geqslant 0 \tag{B.2}$$

which is exact at $x = 0$. Then

$$I_5(a,b,\Theta) \leqslant \frac{2/\sqrt{\pi}}{b\Theta+\sqrt{b^2\Theta^2+4/\pi}}\int_{\Theta}^{\infty}\mathrm{e}^{-(a^2+b^2)w^2}\,\mathrm{d}w = \frac{\mathrm{erfc}(d\Theta)}{d(b\Theta+\sqrt{b^2\Theta^2+4/\pi})} \tag{B.3}$$

References

[1] P.J. Roach, Verification and Validation in Computational Science and Engineering, Hermosa, Albuquerque, NM, 1998.

[2] R.L. McMasters, Z. Zhou, K.J. Dowding, C. Somerton, J.V. Beck, Exact solution for nonlinear thermal diffusion and its use for verification, AIAA J. Thermophys. Heat Transfer 16 (2) (2002) 366–372.

[3] J. Beck, R. McMasters, Verification solutions for heat conduction with solid body motion and isothermal boundary conditions, Arab. J. Sci. Eng. 27 (2002) 49–65.

[4] J. Beck, R. McMasters, Solutions for multi-dimensional transient heat conduction with solid body motion, Int. J. Heat Mass Transfer, in press.

[5] R. McMasters, K. Dowding, J. Beck, D. Yen, Methodology to generate accurate solutions for verification in transient three-dimensional heat conduction, J. Numer. Heat Transfer B 41 (2002) 521–541.

[6] D.H.Y. Yen, J. Beck, R. McMasters, D.E. Amos, Solution of an initial-boundary value problem for heat conduction in a parallelepiped by time partitioning, Int. J. Heat Mass Transfer 45 (2002) 4267–4279.

[7] J.V. Beck, K. Cole, A. Haji-Sheikh, B. Litkouhi, Heat Conduction Using Green's Function, Hemisphere Press, New York, 1992.

[8] G. Myers, Analytical Methods in Conduction Heat Transfer, McGraw-Hill, New York, 1971.

[9] K.D. Cole, D.H.Y. Yen, Green's functions temperature and heat flux in the rectangle, Int. J. Heat Mass Transfer 44 (2001) 3883–3894.

[10] P.E. Crittenden, K.D. Cole, Fast-converging steady-state heat conduction in the rectangular parallelepiped, Int. J. Heat Mass Transfer 45 (2002) 3585–3596.

[11] D.E. Amos, Integrals related to heat conduction and diffusion, Beck Engineering Consultants Co. for Sandia National Laboratories, August 2003. Available from <http://www.beckeng.com>.

[12] D.E. Amos, Computation of exponential integrals, ACM Trans. Math. Softw. 6 (3) (1980) 365–377.

[13] D.E. Amos, Algorithm 556 Exponential integrals [S13], ACM Trans. Math. Softw. 6 (3) (1980) 420–428.

[14] M. Abramowitz, I.A. Stegun, Handbook of Mathematical Functions, National Bureau of Standards, Applied Math Series, vol. 55, 1964.